Hindawi Publishing Corporation
Journal of Nanomaterials
Volume 2016, Article ID 2192647, 10 pages
http://dx.doi.org/10.1155/2016/2192647

Research Article

Supercritical CO_2 Assisted Synthesis of EDTA-Fe_3O_4 Nanocomposite with High Adsorption Capacity for Hexavalent Chromium

Gunjan Bisht,[1] Sanjila Neupane,[2] and Rebika Makaju[3]

[1]*Department of Chemical Science and Engineering, Kathmandu University, Dhulikhel, Nepal*
[2]*Department of Environmental Science and Engineering, Kathmandu University, Dhulikhel, Nepal*
[3]*Department of Natural Science, Kathmandu University, Dhulikhel, Nepal*

Correspondence should be addressed to Gunjan Bisht; gunjanbisht31@gmail.com

Received 27 June 2016; Revised 27 October 2016; Accepted 31 October 2016

Academic Editor: Paulo Cesar Morais

Efficiency of EDTA functionalized nanoparticles in adsorption of chromium (VI) from water was investigated in this study. Magnetic iron oxide nanoparticles (IONPs) were synthesized by a simple chemical coprecipitation route and EDTA coating onto IONPs was attained via supercritical carbon dioxide (Sc CO_2), a technology with green sustainable properties. The obtained nanoparticles were then characterized by UV-Visible spectroscopy, Fourier transform infrared spectroscopy (FTIR), X-ray powder diffraction (XRD), transmission electron microscopy (TEM), scanning electron microscopy (SEM), and vibrating magnetometric analysis (VSM). The synthesized nanoparticle and its modified variant were evaluated as adsorbent for chromium (VI) removal from water through batch adsorption technique and the effect of analytic concentration; contact time and adsorbent concentration were studied at pH 2. The results showed higher removal efficiency for modified magnetic iron oxide nanoparticles (MIONPs) (i.e., 99.9%) than their nonmodified variant IONPs, that is, 34.06% for the same concentration after 18 hours of incubation. Also maximum adsorption capacity (q_e = 452.26 mg/g) of MIONPs attained can be related to their preparation in Sc CO_2 as q_e calculated from IONPs, that is, 170.33 mg/g, is lower than that of MIONPs. The adsorption data fit well with Freundlich isotherm equation while kinetic adsorption studies of chromium (VI) were modeled by pseudo-second-order model.

1. Introduction

Rapid urbanization and industrialization have led to discharging heavy metals in the environment, which are threat to the health of humans as well as the natural ecosystem [1]. These pollutants are causing public health problems due to bioaccumulation, nonbiodegradability, and toxicity even at low concentrations [2]. Thus, various efforts are considered in order to cope with the mortifying status. Chromium (VI) is carcinogenic which imparts threat to environment and humans. Its contamination in drinking water is a burning problem faced by today's world. Thus, WHO recommends permissible limit of chromium (VI) in drinking water to be 50 ppm. Conventional measures like reduction, chemical precipitation, ion exchange, reverse osmosis, and electrochemical treatment are common measures used for removal of heavy metal content in water [3, 4]. However, these methods show drawbacks in their cost, complexity, efficiency, or sludge generation in application at large scale. Thus, adsorption is one promising technology outstanding among all other methods because of its simple design, ease in operation, low cost, and high retention efficiency when applied with proper adsorbent [5–7].

Several materials, such as activated carbons, clay minerals, chelating materials, and chitosan/natural zeolites, have been researched to adsorb heavy metal ions from aqueous solutions. Also low cost biosorbents such as agricultural wastes, clay materials, biomass, and seafood processing waste are used as they are inexpensive and are capable of removing trace level of heavy metals in water [8]. However, applications of these sorbents are limited as these are not as effective as nanomaterials. After extensive study on nanomaterials for

over a decade, it has been proved that nanomaterials have noble and unique properties and wide range of applications thus are potential enough for environment cleanup and preventing environmental pollution [9]. These exhibit higher efficiency and have faster rate in application of treatment of water when compared with other traditional sorbents [5]. Important characteristics of nanoparticles, which made them ideal adsorbents, are small size, catalytic potential, high reactivity, large surface area, ease of separation, and large number of active sites for interaction with different contaminants. These properties are responsible for high adsorption capacities by increasing the surface area, free active valences, and surface energies of nanoparticles.

Thus, the objective of this research was to develop simpler and versatile approach using IONPs and comparative study of these with MIONPs for removal of chromium (VI) from water. Modification of nanoparticles can be done by attaching suitable functional groups such as carboxylic acids, phosphoric acid, silanol, thiol, and amine or small organic molecules, biomolecules, polymer, ligands, and other nanoparticles increasing adsorption capacity that improves its activity and hence its efficiency [10, 11]. However, use of various solvents imposes some sort of toxicity even after purification so Sc CO_2 was used for surface modification of IONPs as it is environmentally benign process. Various studies relating synthesis of nanoparticles via Sc CO_2 are in biomedical application mostly for drug delivery and therapeutic study [12]; however, only a handful are there in environmental aspects. Usage of Sc CO_2 reactor system in processing of nanocomposites for studies related to environmental aspects bear tremendous opportunities as it is antisolvent process that restricts the use of solvents associated with conventional modification method. It turns out to be effective and efficient process when dealing with drinkable thing like water that requires use of minimum toxicants. Also this favors the principle of recycling wastes as it uses one of the abundant greenhouse gases, carbon dioxide in the synthesis process. This could be one of the efficient ways to capture and reuse the wasted gas that is generated in enormous volume every year.

Among different nanostructures used for treatment of water, magnetic iron oxide nanoparticle was used in this research. Its properties such as strong adsorption capacity, good stability, unique magnetic properties, and insignificant toxicity facilitates extensively in environmental remediation [13]. Also it exhibits superparamagnetic behavior favoring fast magnetic separation in aqueous solution and increases reuse of adsorbent [14] and thus is established as most preferred one in water treatment and environment cleanup. IONPs easily aggregate in aqueous solution as they have weak chemical stability against air oxidation and are incapable of retaining adsorption materials. As a result, surface modification is required to stabilize IONPs for their application. Modification in Sc CO_2 enhanced the polymerization process producing MIONPs that enhances the efficiency of chromium (VI) removal from water.

Our aim of the study was to provide an ideal method for synthesis of nanocomposites and their characterization using tools such as UV-Visible spectroscopy, FTIR, XRD, SEM, TEM, and VSM. A study of different parameters like concentration, contact time, and adsorbent dosage was conducted to obtain optimum condition required for removal of chromium (VI). The adsorption isotherm and adsorption kinetics were established to explain mechanism of adsorption process.

2. Materials and Methods

2.1. Synthesis of IONPs and MIONPs. IONPs comprising selected particle size were synthesized by usual chemical coprecipitation method using ammonia as precipitating agent. IONPs were prepared by gradual addition of ammonium hydroxide (7.0 M, 50 mL) at the rate of 1 cc/sec to the aqueous solution containing different concentrations of $FeCl_2 \cdot 4H_2O$ at 90°C. The precipitate obtained was filtered and dried overnight at room temperature to yield IONPs with different IONPs crystallite size and magnetic properties [12]. The EDTA modification of IONPs was carried out in a stainless steel high pressure compact reactor (100 cm^3), model 5513, equipped with a PID temperature controller, manufactured by Parr Instrument Company, Illinois, USA. A requisite mixture of 10 mL of distilled water solution of EDTA (1 g) and IONPs (0.1 g) was prepared by vortexing and by ultrasonication that charged the reactor. The reaction mixture was gradually heated with electrically heating tape wrapped around the exterior wall of the cell at 80 ± 1°C to obtain the desired pressure of 1200 psi. Then, the reaction mixture was allowed to reflux over 6 hours. The CO_2 was vented into dichloromethane from the cell at 25 ± 1°C and modified IONPs were obtained with yield (%) 84.7 [12, 15].

2.2. Characterization. Nanoparticle properties are generally characterized by their size, morphology, and surface charge, using advanced techniques since they vary significantly with size and shapes [16]. The prepared IONPs and MIONPs were characterized through spectral analysis (UV spectra, FTIR, and XRD), microscopic analysis (SEM and TEM), and vibrating magnetometric analysis (VSM). The concentration of chromium (VI) was determined by UV-Visible spectra recorded in water using spectrophotometer model Genesis 10 Thermo Scientific, USA, at the increment of 3 nm. Transmission electron microscopy (TEM) images were recorded at 4-KX and 50x magnification and 1 μm and 100 μm scale over JEOL 1011 (Tokyo, Japan). Scanning electron microscopy (SEM), a high resolution microscopic technique, provided surface morphology of nanoparticles at 100 nm and 200 nm scale [17]. The magnetic magnetization property of nanoparticles was obtained by vibrating sample magnetometer (VSM) Princeton EG & G applied research model 155 with maximum current 30 A, reading number 150, and scan time 900 s at room temperature. The Fourier transformed-infrared (FTIR) spectra were recorded over Shimadzu 8400 spectrophotometer in KBr performed on dried samples with resolution 4 cm^{-1} which generated corresponding spectrum using IR-Solution software. The synthesized particles were characterized using X-ray diffraction (XRD) using Cu k α radiation of wavelength 1.54056°A with range 2θ from 20° to 80° and scan rate of 10/min [17].

2.3. Adsorption Study. Batch adsorption experiments of the chromium (VI) adsorption using IONPs and MIONPs were carried out at room temperature and conducted in acidic environment, at pH 2 [18–20] by shaking a series of bottles each containing the desired quantity of the adsorbent in a predetermined concentration of chromium (VI) in solution. Different parameters in samples examined include initial amount of IONPs, reaction time, and initial concentration of chromium (VI). To perform experiments, $K_2Cr_2O_7$ (1 g/L) solution and various dilutions of its chromium (VI) solution were prepared. For each test, nanoadsorbents were separated by external magnetic field and analysis for remaining chromium (VI) content was done using UV-Visible spectrophotometer [11, 20, 21]. The percent removal of chromium (VI) from solution was calculated by the following equation:

$$\% \text{ Adsorption} = \frac{100 * (C_o - C_e)}{C_o}, \quad (1)$$

where C_o is initial concentration of chromium (VI) and C_e is final concentration of chromium (VI).

Adsorption studies of chromium (VI) on nanoparticles were carried out at optimum pH 2 because, at pH range 2–2.5, these have maximum removal efficiency of chromium (VI). Different species of chromium (VI) coexist at acidic pH among which predominant species (HCrO4–) is favorably adsorbed at this range since it has low adsorption-free energy [19, 20]. Beside these, adsorption capacity and adsorption behavior of chromium (VI) on nanoparticles can be illustrated by adsorption isotherm. Each of the models, that is, Langmuir, Freundlich, and Temkin, has variations in type of system and adsorption modes. Kinetic performance of an adsorbent indicates solute uptake rate; thus, kinetic study was performed to determine residence time required to complete adsorption reaction [18]. Two kinetic models (pseudo-first-order and pseudo-second-order) were applied to fit kinetic data [19].

3. Result and Discussion

3.1. Characterization. The synthesized IONPs and MIONPs were prepared for the UV-Visible analysis by preparing stock solutions of samples of concentration 10 mg/mL in water. Each solution of 10 mg/mL IONPs and MIONPs prepared in water was diluted to appropriate concentration and absorbance was measured from wavelength 200 nm to wavelength 600 nm using UV-Visible spectrophotometer. The UV-Visible absorption spectrum recorded for the respective samples are shown in Figure 1. The IONPs showed no measurable features in the visible region other than maximum absorption at 264 nm, while the MIONPs displayed a surface plasmon resonance band at 232 nm. On comparison, peak corresponding to absorption due to IONPs showed hypsochromic shift (blue shift).

FTIR spectra determined specific functionality of nanoparticles and verified the combination of Fe_3O_4 with EDTA (Figure 2). FTIR spectra of IONPs and MIONPs showed broad peaks at 561.28 cm^{-1} and 545.85 cm^{-1} due to the stretching vibrations of Fe (II)-O and Fe (III)-O bonds.

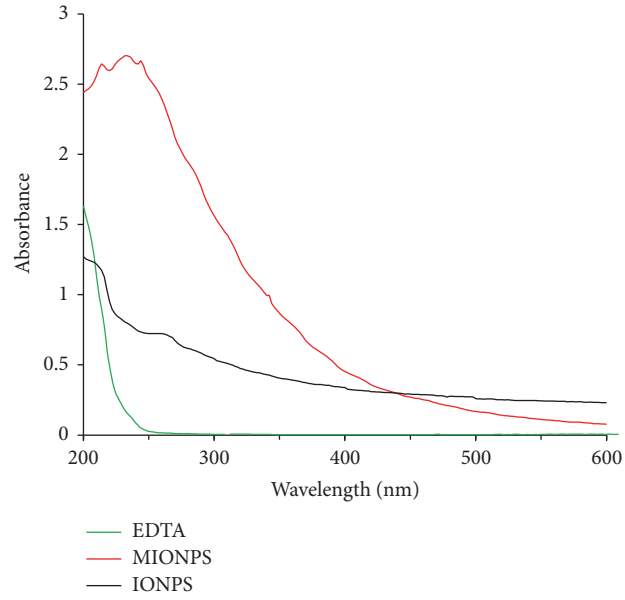

Figure 1: UV-Visible spectra of IONPs, EDTA, and MIONPs.

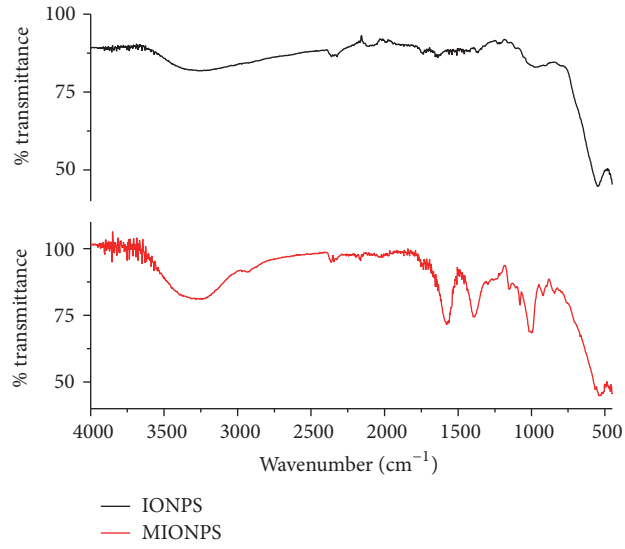

Figure 2: Ftir spectra of IONPs and MIONPs.

In the spectrum for MIONPs, absorption band at 3261.62 cm^{-1} is stretching O–H bond due to intercalated water molecules [22]. After functionalization with EDTA, new characteristic peaks of C=O at 1629.84 cm^{-1} and C-H_2 at 1284.59 cm^{-1} and the stretching vibration of C-N bond at 1018.41 cm^{-1} were observed suggesting introduction of EDTA onto Fe_3O_4.

XRD is used to study the crystal structure of solids. XRD patterns of IONPs and MIONPs are shown in Figure 3. MIONPs (IONPs) showed diffraction peaks corresponding to hkl at 110, 200, 202, 210, and 113 at 2θ values at 35.528 (35.687), 42.546 (43.25), 54.301 (53.434), 57.119 (57), and 62.614 (62.739) indicating their magnetite structure. Compared to the diffraction peak intensities of IONPs, slight decrease in peak

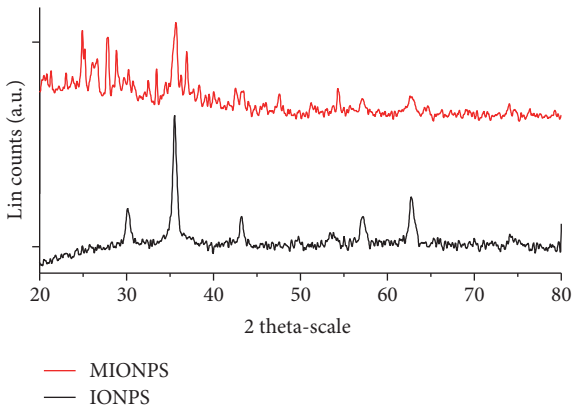

Figure 3: XRD spectra of IONPs and MIONPs showing peaks at 2θ values from 20° to 80°.

intensities of MIONPs was seen probably due to the surface modification. However, there was no change in the peak position which indicates that IONP maintained its crystalline structure even after surface modification [19].

SEM and TEM analysis revealed the microscopic structure of nanoparticles (Figure 4). TEM images and size distribution of IONPs in the different scale of 100 nm and 200 nm showed particles aggregated in lumps due to their magnetic nature [11]. Also the particle size of about 20 nm was observed for the synthesized IONPs. SEM images at different scale from 1 and 100 μm revealed the clear macro granules of ligand moiety dispersed on IONPs surface. The surface modification of IONPs with crystalline EDTA had irregularly dispersed resulting to increase in size [11].

The study of magnetic behavior of IONPs and MIONPs along with their magnetization measurements was recorded. M-H hysteresis curves of IONPs and MIONPs are shown in Figure 5. The magnetic behavior of materials depends on many factors, such as elemental composition, crystallinity, shape, size, and orientation. In agreement with the predictions of the particle size from SEM, TEM, and XRD data, it can be found that, with increase in the particle size, IONPs show higher coercivity (126 Oe) over MIONPs (25 Oe) with simultaneous decrease in their remanence of 0.05 emu/g and 6.61×10^{-4} emu/g, respectively. Further, this contributed reduction in the saturation magnetization (emu/g) of MIONPs (0.1658) over IONPs (47.25) [23]. Thus, IONPs showed higher magnetization compared to MIONPs.

3.2. Effect of Adsorbent Dosage on Adsorption of Chromium (VI). Figure 6 shows the effect of adsorbent dosage on removal of chromium (VI) from aqueous medium. These studies were carried out on equilibrium concentration: time 180 minutes and pH 2. The results showed that q_e increased with increase in concentration of absorbent; however, for the same concentration of absorbent, q_e value for MIONPs varies from 320.17 mg/g to 499.5 mg/g which is comparatively greater than that for IONPs, that is, 86.88 mg/g to 170.33 mg/g.

After 18 h, the observed removal efficiency of chromium (VI) by MIONPs at initial concentration of 5, 10, 15, 20, 25, and 30 mg/L was 64.03%, 77.67%, 89.16%, 93.77%, 96.65%, and 99.90%, respectively, while for IONPs it was 17.37%, 19.15%, 22.41%, 25%, 29.05%, and 34.06%, respectively. Also the Sc CO_2 synthesized MIONPs showed better increased adsorption capacity compared to the MIONPs synthesized from conventional techniques as reported in similar studies [24, 25].

3.3. Effect of Contact Time on Adsorption of Chromium (VI). Experiments were run with the initial concentration of chromium (VI) at 1000 mg/L, while varying the contact time from 0 to 180 min with an adsorbent dose of 10 mg. The extent of removal of chromium (VI) by IONPs and MIONPs increased with the increase in contact time (Figure 7). However, the adsorption was faster at the initial stage than the later stage due to the availability and plenty of active sites on the adsorbent surface. After 3 hours, MIONPs could adsorb up to 163.97 mg/g of adsorbate while unmodified IONPs could adsorb up to 147.95 mg/g of adsorbate. Variation and effectiveness of MIONPs can also be seen in the result obtained after 18 hours of incubation; that is, MIONPs adsorbed 452.26 mg/g of adsorbate while IONPs could adsorb 170.33 mg/g of adsorbate.

3.4. Effect of Initial Concentration on Adsorption of Chromium (VI). The effect of initial concentration (200 to 1000 mg/L) of chromium (VI) adsorption on IONPs and MIONPs surfaces is presented in Figure 8 showing their adsorption capacities. For IONPs and MIONPs, the q_e value increased as a function of increase concentration of chromium (VI). The value ranges from 82.80 to 367.67 mg/g for MIONPs and, for IONPs, it ranges from 37.55 to 106.33 mg/g. Thus, MIONPs have greater adsorption efficiency than IONPs as they are enhanced by their modification with EDTA in Sc CO_2.

3.5. Adsorption Kinetic Study. In order to understand the kinetic mechanism of adsorption phenomena of chromium (VI) by nanoparticles, two kinetic models, that is, pseudo-first-order and pseudo-second-order, were applied to fit kinetic data. A pseudo-first-order equation [19, 24] is in the following form:

$$\log(q_e - q_t) = \log q_e - \frac{k_1}{2.303t}, \tag{2}$$

where q_t is the amount of adsorbate adsorbed at time t (mg g^{-1}), q_e is the adsorption capacity in the equilibrium (mg g^{-1}), k_1 is the pseudo-first-order rate constant (min^{-1}), and t is the contact time (min).

A pseudo-second-order equation [19] based on adsorption equilibrium capacity is expressed in the following form:

$$\frac{t}{q_t} = \frac{1}{k_2 q_e^2} + \left(\frac{1}{q_e}\right) t, \tag{3}$$

where k_2 is the pseudo-second-order rate constant (mg g^{-1} min^{-1}).

The results of adsorption studies carried out as a function of contact time, for chromium (VI), are presented in Figures 9(a) and 9(b). It is suggested that the removal of chromium

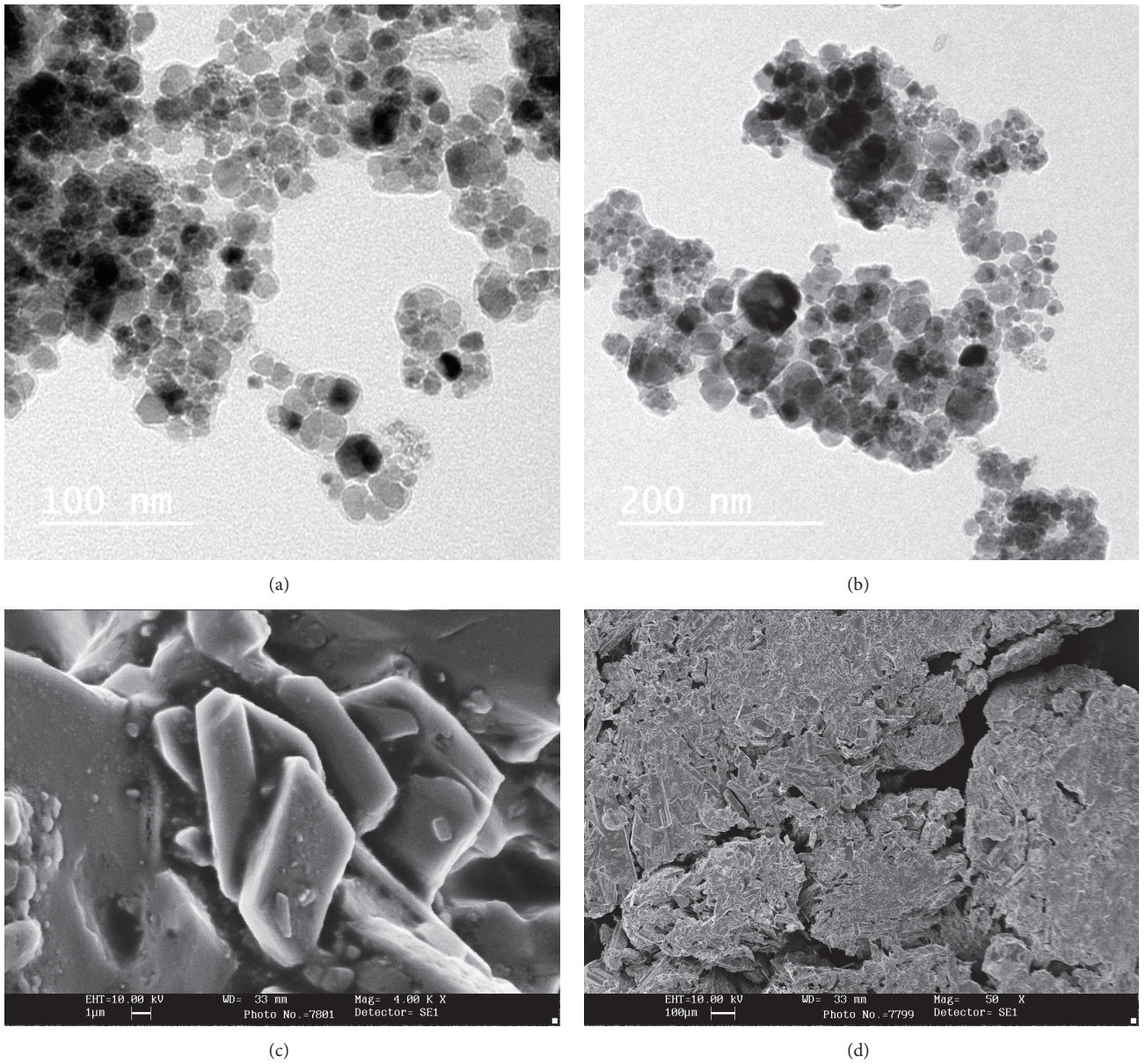

(a) (b)

(c) (d)

Figure 4: Microscopic images of nanoparticles: (a) TEM image of IONPs at 100 nm, (b) TEM image of IONPs at 200 nm, (c) SEM image of MIONPs at 4.00 Kx magnification and 1 μm scale, and (d) SEM image of MIONPs at 50x magnification and 100 μm scale.

(VI) by IONPs and MIONPs adsorbents took place in two distinct steps: a relatively quick phase (first 3 h), followed by a slow increase until the equilibrium was reached. The necessary time to reach the equilibrium was about 18 h.

The kinetics parameters and correlation coefficients were calculated from the linear plots and are listed in Table 1. A low correlation coefficient was observed for the pseudo-first-order model, indicating a poor pseudo-first-order fit to the experimental data for adsorption of chromium (VI) by both IONPs and MIONPs. However, the correlation coefficient for the pseudo-second-order model was higher than the values obtained for pseudo-first-order model. Hence, the adsorption kinetics of chromium (VI) was well described by the pseudo-second-order model.

Table 1: Comparison between pseudo-first-order and second-order kinetic models for chromium (VI) adsorption by IONPs and MIONPs.

Sorbents	First-order		Second-order	
	R^2	K_1 (min^{-1})	R^2	K_2 (g mg^{-1} min^{-1})
IONPs	0.9354	0.0081	0.9642	$1.53*10^{-4}$
MIONPs	0.9996	0.0025	0.9998	$3.17*10^{-6}$

3.6. Adsorption Isotherm. Adsorption capacity and adsorption behavior of chromium (VI) on IONPs and MIONPs can be illustrated by adsorption isotherm. Each of the models, that is, Langmuir, Freundlich, and Temkin, has variations in

Table 2: Langmuir, Freundlich and Temkin isotherm model constant for adsorption of chromium (VI).

Sorbents	Langmuir model			Freundlich model			Temkin model	
	b (Lmg^{-1})	R^2	R_L	K_F (mgg^{-1})	n	R^2	b (J/moL)	R^2
IONPs	0.0023	0.9032	0.456	6.986	1.92	0.9752	0.056	0.9201
MIONPs	0.0039	0.9312	0.339	3.184	1.38	0.9809	0.0013	0.9694

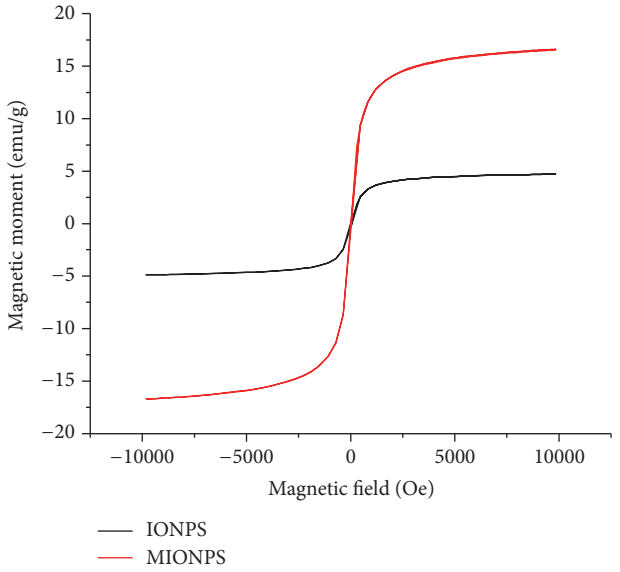

Figure 5: M-H hysteresis curves of IONPs and MIONPs.

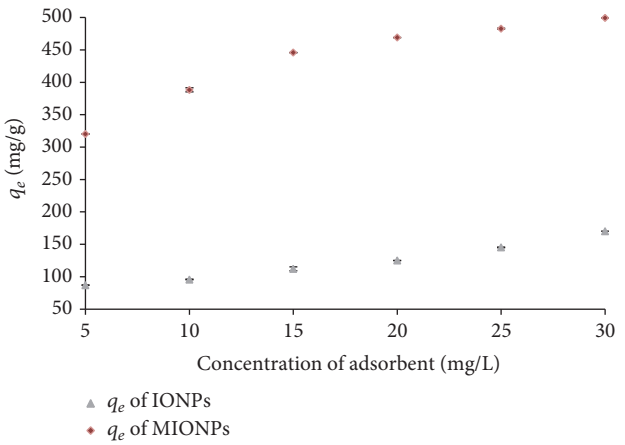

Figure 6: Effect of absorbent dosage for adsorption of chromium (VI) on IONPs and MIONPs at equilibrium concentration, time of 180 minutes, pH 2, and room temperature.

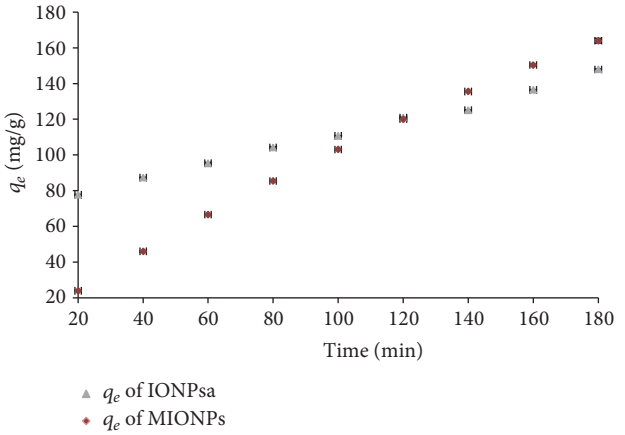

Figure 7: Effect of contact time for adsorption of chromium (VI) on IONPs and MIONPs at initial concentration 1000 mg/L, adsorbent dosage 10 mg, pH 2, and temperature 298 K.

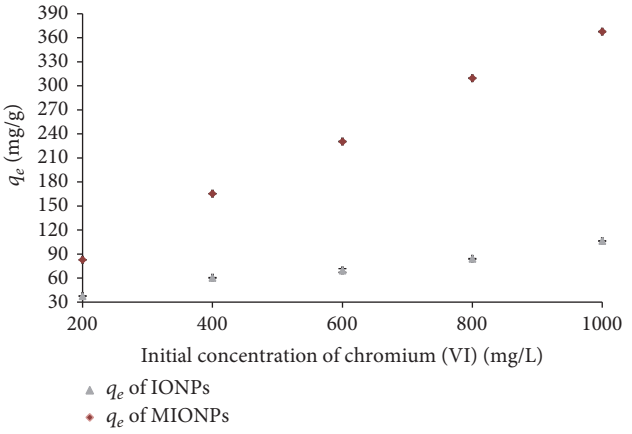

Figure 8: Effect of initial concentration of chromium (VI) for adsorption on IONPs and MIONPs at different initial concentration (200–1000 mg/L), time 180 minutes, pH 2, and temperature 298 K.

type of system and adsorption modes. The fitted constants for adsorption isotherms along with regression coefficients are summarized in Table 2 configured from Figure 10. The adsorption of chromium (VI) was observed in the pH 2.

Langmuir isotherm equation is derived from monolayer adsorption with the assumption that the adsorbent surface has a fixed number of equivalent binding sites and without transmigration of adsorbate on the surface of adsorbent isotherm [26, 27]. Graphically, it is represented by a plateau, an equilibrium saturation point where once a molecule occupies a site, no further adsorption can take place [27, 28].

The Langmuir equation can be written as

$$q_e = \frac{(q_m b C_e)}{(1 + bC_e)}. \quad (4)$$

The linearized form of Langmuir can be written as

$$\frac{C_e}{q_e} = \frac{1}{(q_m b)} + \frac{C_e}{q_m}, \quad (5)$$

where q_e is the solid-phase equilibrium concentration (mg g^{-1}); C_e is the liquid equilibrium concentration of

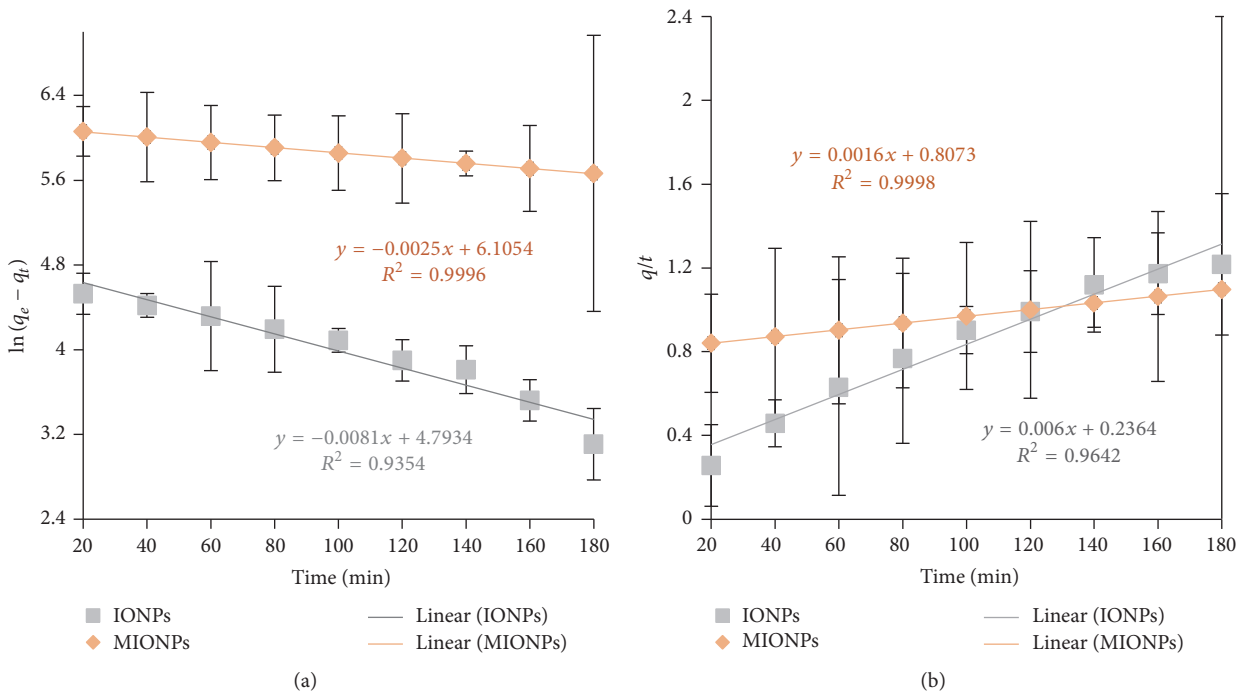

FIGURE 9: (a) Pseudo-first-order kinetics for adsorption of chromium (VI) on IONPs and MIONPs and (b) pseudo-second-order kinetics for adsorption of chromium (VI) on IONPs and MIONPs.

chromium (VI) in solution (mg L^{-1}); b is the equilibrium constant related to the affinity of binding site (L mg^{-1}); and q_m is the maximum amount of the chromium (VI) per unit weight of adsorbent for complete monolayer coverage [5].

After equilibrium, the adsorption capacity q_e (mg/g) was calculated using a mass balance relationship equation:

$$q_e = \frac{(C_o - C_e)V}{W}, \tag{6}$$

where C_o is the initial concentration of test solution (mg/L) and C_e is the equilibrium concentration of chromium (VI) (mg/L), V is the volume of the solution (L), and W is the mass of adsorbent (g) [4].

R_L, a dimensionless constant separation factor, determines whether a Langmuir adsorption system is favorable or not. The favorability of the absorption isotherm is defined for specific R_L values as for R_L >1 unfavorable, R_L =1 is linear, R_L between 0 and 1 is favorable, and R_L =0 irreversible [27]. The separation factor, R_L, is defined as follows:

$$R_L = \frac{1}{(1 + bC_o)}, \tag{7}$$

where C_o is the initial concentration of chromium (VI) and b is the Langmuir adsorption constant (L mg^{-1}).

The constants of Langmuir isotherm, b and C_o, are greater than 0 and the value of R_L lies within the range of 0-1 (Table 2) as shown in Figures 10(a) and 10(b) indicating the adsorption of chromium (VI) on nanoparticles which is highly favorable under the experimental condition used in this study [27].

The Freundlich isotherm was chosen to estimate the adsorption intensity of the adsorbent towards the adsorbate. The Freundlich isotherm is empirical model that is based on sorption on a heterogeneous surface allowing multilayer adsorption on sorbent.

The nonlinear form of Freundlich isotherm is

$$q = K_F C_e q^{1/n}, \tag{8}$$

where $C_e q$ is the equilibrium concentration (mg/L) and q is the amount adsorbed (mg/g). K indicates the relative adsorption capacity of the adsorbent and n represents the adsorption intensity. Linearly, the Freundlich isotherm is expressed as

$$\ln q_e = \ln K_F + \frac{1}{n \ln C_e}. \tag{9}$$

The Freundlich constant, n, can be used to predict the adsorption characteristics. If the n value is equal to 1, then adsorption is linear; if $n < 1$, then adsorption is a chemical process; if $n > 1$, then adsorption is a physical process. The values of n within the range of 1–10 represent good adsorption [29, 30]. The constant n in Freundlich equation was found to be 1.92 and 1.38 for IONPs and MIONPs (Table 2) (Figures 10(c) and 10(d)). As n lies between 1 and 10, it indicates the physical adsorption of chromium (VI) onto IONPs and MIONPs [31, 32].

The Temkin isotherm [24, 33] equation is generally applied in the following form:

$$q_e = \left(\frac{RT}{b}\right) \ln (AC_e). \tag{10}$$

This can be linearized as

$$q_e = B \ln A + B \ln C_e, \tag{11}$$

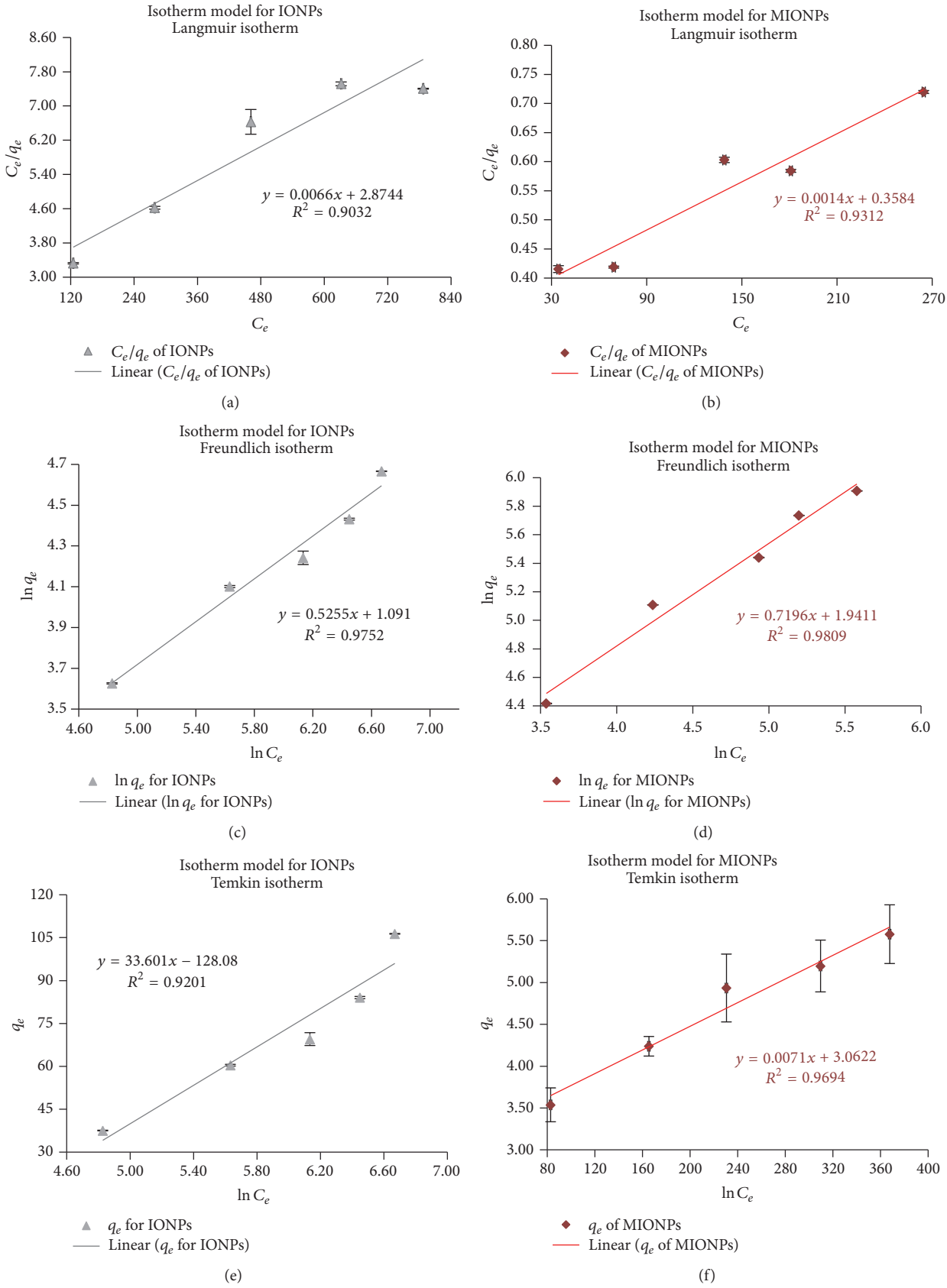

Figure 10: Different adsorption isotherm for chromium (VI) on IONPs and MIONPs.

where $B = RT/b$, b is the Temkin constant related to heat of sorption (J/moL), A is the Temkin isotherm constant (L/g), R is the gas constant(8.314 J/moL K), and T is the Kelvin temperature (K).

For Temkin isotherm, the value of A and b were obtained by the plotting of q_e versus $\ln C_e$ [27, 31] shown in Figures 10(e) and 10(f).

Comparing R^2 values for three isotherms, Freundlich isotherm has the highest value of R^2; thus, the adsorption of chromium (VI) by nanoparticles fits better with Freundlich isotherm.

4. Conclusion

MIONPs were synthesized via Sc CO_2 for adsorption process and were employed in the removal of chromium (VI) in water treatment. The removal efficiency of IONPs was compared with the modified IONPs that were synthesized using a chelating ligand, EDTA. When IONPs and MIONPs were used as adsorbent in chromium removal, MIONPs could remove up to 99.90% chromium from sample while IONPs could remove only about 34.06%. Also the MIONPs synthesized from supercritical carbon dioxide (Sc CO_2) assisted process increased the adsorption capacity (q_e) relative to that of IONPs. The Langmuir, Freundlich, and Temkin adsorption models were used to express the sorption at pH 2. The Freundlich isotherm has the best fit to the experimental data. Kinetic adsorption studies of chromium (VI) at pH 2 were conducted and pseudo-second-order model described the adsorption kinetics.

Competing Interests

The authors declare that they have no competing interests.

Acknowledgments

The authors acknowledge International Foundation for Science (IFS) cofinanced by the Organization for the Prohibition of Chemical Weapons (OPCW) for support under Grant no. 5580 and The World Academy of Sciences (TWAS) for equipment support purchased under research Grant no. 14-187RG/CHE/AS_I-UNESCO FR: 324028568. In addition, the authors would also like to acknowledge Ms. Pooja Rani for material characterization support.

References

[1] J. Zhu, S. Wei, M. Chen et al., "Magnetic nanocomposites for environmental remediation," *Advanced Powder Technology*, vol. 24, no. 2, pp. 459–467, 2013.

[2] Y. Feng, J.-L. Gong, G.-M. Zeng et al., "Adsorption of Cd (II) and Zn (II) from aqueous solutions using magnetic hydroxyapatite nanoparticles as adsorbents," *Chemical Engineering Journal*, vol. 162, no. 2, pp. 487–494, 2010.

[3] Z. Elouear, J. Bouzid, N. Boujelben, M. Feki, F. Jamoussi, and A. Montiel, "Heavy metal removal from aqueous solutions by activated phosphate rock," *Journal of Hazardous Materials*, vol. 156, no. 1–3, pp. 412–420, 2008.

[4] A. M. Mahmoud, F. A. Ibrahim, S. A. Shaban, and N. A. Youssef, "Adsorption of heavy metal ion from aqueous solution by nickel oxide nano catalyst prepared by different methods," *Egyptian Journal of Petroleum*, vol. 24, no. 1, pp. 27–35, 2015.

[5] X. Wang, Y. Guo, L. Yang, M. Han, J. Zhao, and X. Cheng, "Nanomaterials as Sorbents to remove heavy metal ions in wastewater treatment," *Journal of Environmental & Analytical Toxicology*, vol. 2, article 7, 2012.

[6] S. D. S. dos Melo, J. E. M. de Diniz, J. H. Guimarães et al., "Production and characterization of absorbent heat from the bark of residual Brazil nut bark (*Bertholletia Excelsa* l.)," *Chemistry Central Journal*, vol. 9, no. 1, article 36, 2015.

[7] Y. Cao and X. Li, "Adsorption of graphene for the removal of inorganic pollutants in water purification: a review," *Adsorption*, vol. 20, no. 5-6, pp. 713–727, 2014.

[8] A. Farghali, M. Bahgat, A. Enaiet Allah, and M. Khedr, "Adsorption of Pb(II) ions from aqueous solutions using copper oxide nanostructures," *Beni-Suef University Journal of Basic and Applied Sciences*, vol. 2, no. 2, pp. 61–71, 2013.

[9] L. Giraldo, A. Erto, and J. C. Moreno-Piraján, "Magnetite nanoparticles for removal of heavy metals from aqueous solutions: synthesis and characterization," *Adsorption*, vol. 19, no. 2–4, pp. 465–474, 2013.

[10] P. N. Dave and L. V. Chopda, "Application of iron oxide nanomaterials for the removal of heavy metals," *Journal of Nanotechnology*, vol. 2014, Article ID 398569, 14 pages, 2014.

[11] E. Alzahrani, "Gum Arabic-coated magnetic nanoparticles for methylene blue removal," *International Journal of Innovative Research in Science, Engineering and Technology*, vol. 3, no. 8, pp. 15118–15129, 2014.

[12] G. Bisht and M. G. H. Zaidi, "Supercritical synthesis of poly (2-dimethylaminoethyl methacrylate)/ferrite nanocomposites for real-time monitoring of protein release," *Drug Delivery and Translational Research*, vol. 5, no. 3, pp. 268–274, 2015.

[13] P. Xu, G. M. Zeng, D. L. Huang et al., "Use of iron oxide nanomaterials in wastewater treatment: a review," *Science of the Total Environment*, vol. 424, pp. 1–10, 2012.

[14] T. M. Do and Y. J. Suh, "Removal of aqueous Cr(VI) using magnetite nanoparticles synthesized from a low grade iron ore," *The Journal of Korean Association for Particle and Aerosol Research*, vol. 9, no. 4, pp. 221–230, 2013.

[15] N. Neyaz, M. S. S. Zarger, and W. A. Siddiqui, "Synthesis and characterisation of modified magnetite super paramagnetic nano composite for removal of toxic metals from ground water," *International Journal of Environmental Science*, vol. 5, no. 2, 2014.

[16] S. L. Pal, U. Jana, P. K. Manna, G. P. Mohanta, and R. Manavalan, "Nanoparticle: an overview of preparation and characterization," *Journal of Applied Pharmaceutical Science*, vol. 1, no. 6, pp. 228–234, 2011.

[17] K. C. Biplab, S. N. Paudel, S. Rayamajhi et al., "Enhanced preferential cytotoxicity through surface modification: synthesis, characterization and comparative in vitro evaluation of TritonX-100 modified and unmodified zinc oxide nanoparticles in human breast cancer cell (MDA-MB-231)," *Chemistry Central Journal*, vol. 10, no. 1, 2016.

[18] N. lankoonInt, "Use of iron oxide magnetic nanosorbents for Cr (VI) removal from aqueous solutions: a review," *Journal of Engineering Research and Applications*, vol. 4, no. 10, pp. 55–63, 2014.

[19] X. B. Fang, Z. Q. Fang, P. K. E. Tsang, W. Cheng, X. M. Yan, and L. C. Zheng, "Selective adsorption of Cr(VI) from aqueous

solution by EDA-Fe_3O_4 nanoparticles prepared from steel pickling waste liquor," *Applied Surface Science*, vol. 314, pp. 655–662, 2014.

[20] P. Yuan, D. Liu, M. Fan et al., "Removal of hexavalent chromium [Cr(VI)] from aqueous solutions by the diatomite-supported/unsupported magnetite nanoparticles," *Journal of Hazardous Materials*, vol. 173, no. 1–3, pp. 614–621, 2010.

[21] D. Kim and J. Om, "Direct spectroscopic determination of aqueous phase hexavalent chromium," *Universal Journal of Engineering Science*, vol. 1, no. 1, pp. 1–4, 2013.

[22] M. Seyedsadjadi, S. E. Babaei, and N. Farhadyar, "Preparation of surface modified magnetic iron oxide nanoparticles and study of their colloidal behavior," *International Journal of Nano Dimension*, vol. 5, no. 3, pp. 279–284, 2014.

[23] Y. Wei, B. Han, X. Hu, Y. Lin, X. Wang, and X. Deng, "Synthesis of Fe_3O_4 Nanoparticles and their magnetic properties," *Procedia Engineering*, vol. 27, pp. 632–637, 2012.

[24] H. I. Adegoke, F. AmooAdekola, O. S. Fatoki, and B. J. Ximba, "Adsorption of Cr (VI) on synthetic hematite (α-Fe_2O_3) nanoparticles of different morphologies," *Korean Journal of Chemical Engineering*, vol. 31, no. 1, pp. 142–154, 2014.

[25] Y.-G. Zhao, H.-Y. Shen, S.-D. Pan, and M.-Q. Hu, "Synthesis, characterization and properties of ethylenediamine-functionalized Fe_3O_4 magnetic polymers for removal of Cr(VI) in wastewater," *Journal of Hazardous Materials*, vol. 182, no. 1–3, pp. 295–302, 2010.

[26] K. Y. Foo and B. H. Hameed, "Insights into the modeling of adsorption isotherm systems," *Chemical Engineering Journal*, vol. 156, no. 1, pp. 2–10, 2010.

[27] W. Jiang, M. Pelaez, D. D. Dionysiou, M. H. Entezari, D. Tsoutsou, and K. O'Shea, "Chromium(VI) removal by maghemite nanoparticles," *Chemical Engineering Journal*, vol. 222, pp. 527–533, 2013.

[28] S. J. Allen, G. Mckay, and J. F. Porter, "Adsorption isotherm models for basic dye adsorption by peat in single and binary component systems," *Journal of Colloid and Interface Science*, vol. 280, no. 2, pp. 322–333, 2004.

[29] M. B. Desta, "Batch sorption experiments: langmuir and freundlich isotherm studies for the adsorption of textile metal ions onto Teff straw (*Eragrostis tef*) agricultural waste," *Journal of Thermodynamics*, vol. 2013, Article ID 375830, 6 pages, 2013.

[30] S. Hashemian, H. Saffari, and S. Ragabion, "Adsorption of cobalt(II) from aqueous solutions by Fe_3O_4/bentonite nanocomposite," *Water, Air, and Soil Pollution*, vol. 226, no. 1, article 2212, 2015.

[31] H. Zheng, D. Liu, Y. Zheng, S. Liang, and Z. Liu, "Sorption isotherm and kinetic modeling of aniline on Cr-bentonite," *Journal of Hazardous Materials*, vol. 167, no. 1–3, pp. 141–147, 2009.

[32] A. Özer and H. B. Pirinççi, "The adsorption of Cd(II) ions on sulphuric acid-treated wheat bran," *Journal of Hazardous Materials*, vol. 137, no. 2, pp. 849–855, 2006.

[33] F. Najafi, M. Norouzi, K. Zare, and A. Fakhri, "Removal of ethidium bromide by carbon nanotube in aqueous solution: isotherms, equilibrium mechanism studies, and its comparison with nanoscale of zero valent iron as adsorbent," *Journal of Nanostructure in Chemistry*, vol. 3, no. 1, p. 60, 2013.